



**HAL**  
open science

# Validation of the CATHARE 3 code based on Rod Bundle Heat Transfer (RBHT) benchmark data using two-fluid and three-field models

Antoine Du Cluzeau, Philippe Fillion

## ► To cite this version:

Antoine Du Cluzeau, Philippe Fillion. Validation of the CATHARE 3 code based on Rod Bundle Heat Transfer (RBHT) benchmark data using two-fluid and three-field models. NURETH-19 - The 19th International Topical Meeting on Nuclear Reactor Thermal Hydraulics, ANS; IAEA; NRG, Mar 2022, Brussels (online), Belgium. cea-04256708

**HAL Id: cea-04256708**

**<https://cea.hal.science/cea-04256708>**

Submitted on 24 Oct 2023

**HAL** is a multi-disciplinary open access archive for the deposit and dissemination of scientific research documents, whether they are published or not. The documents may come from teaching and research institutions in France or abroad, or from public or private research centers.

L'archive ouverte pluridisciplinaire **HAL**, est destinée au dépôt et à la diffusion de documents scientifiques de niveau recherche, publiés ou non, émanant des établissements d'enseignement et de recherche français ou étrangers, des laboratoires publics ou privés.

# **VALIDATION OF THE CATHARE 3 CODE BASED ON ROD BUNDLE HEAT TRANSFER (RBHT) BENCHMARK DATA USING TWO-FLUID AND THREE-FIELD MODELS**

**Antoine du Cluzeau and Philippe Fillion**

Université Paris-Saclay, CEA, Service de Thermo-hydraulique et de Mécanique des Fluides,  
91191, Gif-sur-Yvette, France.

antoine.ducluzeau@cea.fr; philippe.fillion@cea.fr

## **ABSTRACT**

The Rod Bundle Heat Transfer (RBHT) facility at the Pennsylvania State University has provided data since 2001 for the study and modeling of reflood conditions. The RBHT experiment allows to study predominant phenomena for this kind of transient scenario: effect of the spacer grids, impact of the heat transfers (convection/vaporization/radiation), influence of droplet size and breakups. In the context of a benchmark organized by the OECD/NEA, new data were recently produced, including tests with oscillating boundary conditions, typical of reflooding scenarios. For the CEA, which develops and validates the CATHARE 3 system code, these data are a valuable aid for the development and the validation of reflooding models (interfacial friction, heat transfers, droplet size, film sputtering). The instrumentation of the experiment (which enable to record the clad temperature, the vapor temperature or the droplet diameter) allows a relative separation of the different effects acting on the transient. This article is therefore a validation study of the CATHARE 3 code on the RBHT open test series, using both two-fluid model and the three-field model, where the liquid phase is split into a continuous field and a dispersed field (droplets), implemented in the code. In general, quench front and wall temperatures evolutions are correctly predicted, except for the tests at high reflooding rate. An analysis of models and their limits is proposed, as well as a sensitivity analysis. Particular attention is paid to the differences between the two-fluid model and the three-field model.

## **KEYWORDS**

RBHT, reflood, CATHARE, benchmark, validation

## **1. INTRODUCTION**

CATHARE project has been launched in 1979 by CEA, EDF and FRAMATOME, with the goal to develop a best-estimate thermal-hydraulic code for safety analysis of nuclear reactors. It is mainly used to safety analysis and into real-time simulator of nuclear power plant. It allows to model light water reactors or test facilities using several available modules (0-D, 1-D and 3-D modules). Two-phase flows are described using two-fluid six-equation or three-field nine-equation models. The code allows a three-dimensional (3-D) modeling of the pressure vessel. CATHARE 3 is the new version of the code, developed since 2006 as part of the NEPTUNE project launched by the CEA, EDF, FRAMATOME and IRSN in 2001 [1]. The first industrial version of CATHARE-3 (V2.1) was released in December 2019, in the continuity of the reference version CATHARE-2, and is used for the RBHT benchmark.

The CATHARE reflooding module, available for 1D and 3D modules, has been designed to take into account the physical phenomena occurring near the quench front. In particular, the two-dimensional heat conduction in the heating walls is solved on an additional mesh which follows the quench front [2]. It allows to take into account sudden temperature variations in the streamwise direction. The heat transfer

models have been specifically revised to describe the boiling curve in reflooding conditions (convective heat transfer, nucleate boiling, transition boiling, dispersed flow film boiling, critical heat flux. . . ) as well as the wall heat transfer, droplet diameter and entrainment in the region downstream of the quench front. The calibration and validation of the models has been performed with a large data base from forced reflood analytical experiments in pipes and rod bundles using the 1-D module, the most important were ERSEC [2, 3] in constant reflooding rate and under forced flow oscillations and PERICLES experimental programs.

During the OECD/NEA PREMIUM benchmark and European Commission NURESAFE project, uncertainty quantification of the physical model and propagation of the uncertainties has been carried out using FEBA/SEFLEX and PERICLES-2D tests [4]. The model using the 3-D module of CATHARE is also validated against PERICLES-2D [5] and SCTF [6] reflooding tests. Top-down reflooding model is also available and is validated against PERICLES and REWETT experiments [7].

A three-field model has been implemented in CATHARE-3 [1], including a liquid droplet field, a continuous liquid field and a gas field. This advanced model has been developed in order to improve the flow simulation when liquid droplets and continuous liquid flow at significantly different velocities or temperatures. The first application of the 3-field model of CATHARE-3 was the prediction of the vertical annular-mist flows and dry-out prediction. The three-field model has been first developed for these accidental situations in a Boiling Water Reactor core. Several correlations have been assessed to estimate the entrainment and the deposition in steam-water conditions in pipes [8] [9] [10] and in rod-bundle geometries [11]. Another application of the 3-field model is the simulation of the PWR Large Break Loss of Coolant Accident (LBLOCA). During the reflooding phase of the LBLOCA, small droplets are produced in the core at the quench front. The steam flow carries out these droplets towards the upper plenum the hot legs and the steam generators, where they vaporize, creating the "steam binding" effect which has a big influence on the reflooding rate. In such conditions, 3-field models can be used for the prediction of the behavior of the droplet in the core. In CATHARE 3, the entrainment model has been adapted to these conditions and assessed against PERICLES and previous RBHT reflooding tests at low pressure [12]. For test RBHT 1383, the simulations performed with an older version of CATHARE 3 (V1) showed a fair agreement in the lower part of the bundle but the model did not predict the right quench front velocity at the end of transient, in the upper part above the 6th grid at 2.8 m, where the heat flux decreases. For the test RBHT 1096 at very low pressure (0.138 MPa), the quench front prediction was less accurate than for the test RBHT 1383, and the code underestimated by about 200°C the steam temperature above the quench front in these conditions. In the frame of the European NURESAFE project, University of Pisa assessed and benchmarked three-field model of CATHARE 3 V1.1.13 with the 6-equation model against the FEBA and ACHILLES separate-effect test facilities, both using the 1-D and 3-D modules [13].

A LBLOCA reflooding transient simulated in BETHSY integral test facility under gravity driven conditions was also calculated using the three-field model [12]. In such test, oscillatory reflooding is observed at the beginning of the process and a top-down quenching is rewetting the upper part of the core creating a situation with possible falling films and upward drop flow, which can be better predicted by the 3-field model. One-dimensional models have been also developed and implemented in CATHARE-3 for the entrainment and deposition of the droplets in the hot legs, including both stratified and annular flow regimes [14]. The deposition model takes into account the two mechanisms acting on the droplet deposition in such geometries: turbulent diffusion and gravity. For the latter mechanism, the deposition constant is related to the terminal falling velocity of the droplet, and accounts the droplet diameter, estimated using a specific correlation.

This paper presents results obtained by the CEA, which develops and validates the CATHARE 3 system code, against the 11 open tests of the RBHT benchmark. The data provided by the RBHT experiments are a valuable aid for the development and the validation of reflooding models (interfacial friction, heat transfers, droplet size, film sputtering). One of the main challenge of these open-tests is to validate the CATHARE code on experiments with oscillating or variable flooding conditions and to identify any lack in the physical modeling approach, for future improvements. Thus, a validation study of the CATHARE 3 code on the RBHT open test series has been carried out, using both two-fluid model and the three-field model.

First, a description of the CATHARE code is proposed in section 2. The experiment is described in section 3, followed by the modeling approach used for the simulations. Finally, the results are described in section 4.

## 2. SUMMARY OF REFLOOD MODEL IN CATHARE 3

CATHARE 3 V2.1 includes the revision 6.1 of the physical models of the two-fluid 6-equation model, and, as previously mentioned, a three-field model. These sets of closure laws contain a specific package used in reflooding conditions.

Standard package include features for solving the heat equation in 1-D, in the radial direction of the rod. In order to take into account axial wall temperature steep gradients existing in the vicinity of the quench front, a two-dimensional model for solving the heat equation in the rods is available in CATHARE. A moving 2D meshing is superimposed to the classical 1-D wall calculation and progresses at the velocity of the quench front along the heated structure. The 2D meshing is progressively refined around the quench front in the axial direction of the heat rod, with a typical size of the cells near the quench front around 1 to 0.1 mm, allowing an accurate representation of the heat transfers. A one way coupling method of the 2D conduction module is used with the other modules of CATHARE (hydraulics, 1D conduction wall).

A local specific heat flux is added in the vicinity of the quench front to represent the enhanced heat transfers due to the flow perturbation by the quenching. It is taken proportional to the axial wall temperature, with the aim to account for non-established thermal conditions near the quench front. This term may be very high in a very limited area. The total heat flux  $q_w$  is given by the sum of the standard term (nucleate boiling, film boiling, ...) and the specific heat flux proportional to the axial temperature gradient [7]:

$$q_w = h(T_w - T_{sat}) + K_2 \frac{\delta T_w}{\delta z} \quad (1)$$

where  $h$  is the heat transfer coefficient,  $T_{sat}$  the saturation temperature,  $T_w$  the wall temperature and  $\delta T_w / \delta z$  its axial gradient. The proportionality factor,  $K_2$  coefficient, is a function of pressure, quality and mass flux, calibrated in the code from PERICLES-2D and ERSEC experimental quench front velocity [15]. This additional heat transfer is only applied when the 2D wall meshing is activated. This second term is important at the quench front surrounding where  $DT_w/dz$  is positive and very strong. For other areas of the flow, where  $DT_w/dz$  could be negative for example, this term is negligible compared to the standard heat transfer and thus not important enough to be meaningful on the total heat transfer.

Reflood experiments analyses show that the heat transfer enhancement exists in a more extended but limited area (about 0.2 to 0.5 m [16]) downstream the quench front. It is necessary consider it in order to predict the correct cooldown of the rods, and hence the correct quench time. Violent boiling and liquid sputtering at the quench front and wall-liquid slugs or wall-droplet contacts near the quench front are

possible mechanisms responsible to increase significantly the local heat transfer characteristics, especially for not very high wall temperatures, and thus contribute to a precooling of the rods. Since this type of heat transfer is important only in the vicinity of the quench front, it is not modeled in a phenomenological manner in CATHARE but it is included into a heat transfer enhancement term  $q_{wvi}$  used near the quench front, added to the evaporation flux due to the film boiling:

$$q_{wvi} = F f(\alpha) \max(0, 1 - \frac{\Delta_{ZF}}{\Delta_{Z0}})(T_w - T_{sat}) \quad (2)$$

Parameter  $F$  depends on the geometry (tube or rod-bundle) and  $f$  function of void fraction.  $\Delta_{ZF}$  represents the distance from the quench front, and  $\Delta_{Z0}$  is the maximum distance where the enhancement term acts.

The heat exchange in film boiling  $q_{fb}$  is given by a correlation derived from Berenson [17] model:

$$q_{fb} = (1 - \zeta) \tilde{q}_{Ber} \quad (3)$$

where  $\tilde{q}_{Ber}$  is a modified heat flux from the Berenson model. Parameter  $\zeta$  takes into account, in the inverted slug regime, the possible impacts between the liquid slug and the wall. It represents the time-averaged fraction of the surface covered by the liquid slugs. This fraction has been correlated in terms of a liquid Reynolds number:

$$\zeta = \zeta_1 Re_l^{\zeta_2}. \quad (4)$$

Coefficients  $\zeta_1$  and  $\zeta_2$  are calibrated from PERICLES data [2].

In a two-fluid model as the one used in CATHARE, the vapor de-superheating effect of liquid slugs and drops downstream of the quench front is taken into account by the interfacial heat transfer correlations. The vapor-to-interface heat transfer is in CATHARE a combination of the heat flux in inverse annular flow regime and in dispersed flow regime. In the dispersed flow regime, the vapor-to-interface heat transfer is calculated from

$$Nu(1 + B) = 2 + 0.57 Re_g Pr_g^{0.33}. \quad (5)$$

In the previous equation, the gas Reynolds number depends on the droplet diameter  $\delta$ . At high evaporation rates, the evaporation from the droplet reduces the convective heat transfer. This is because the vapor mass flux leaving the droplet surface goes in the opposite direction of the heat flux from the superheated vapor to the droplet and affects the flow field near the droplet. This heat transfer reduction can be incorporated by dividing the interfacial heat flux by a factor  $(1 + B)$  [18], where  $B$  is the blowing parameter approximated in CATHARE by  $10^{-3}(T_g - T_{sat})$  [19].

For the 6-equation model, the amount of droplets in the core is estimated using a correlation of the entrainment fraction  $E$ . In reflooding conditions, the correlation is derived from:

$$E = \left[ \sin \left( a \left( \frac{J_g}{J_{crit}} \right) - b \right) \right]^m \quad (6)$$

where  $J_g$  is the gas superficial velocity and  $J_{crit}$  is the critical gas superficial velocity at which the entrainment begins. Parameters  $a$ ,  $b$ , and  $m$  are fitted from experimental data. In the case of the three-field model, the amount of droplets results from the mass balance from the 3 fields, and mainly depends on the balance between the entrainment and deposition rates. In reflooding conditions, the entrainment rate  $\Gamma_E$  ( $kg/(m^2 s)$ ) is estimated by a specified correlation, derived but modified in the current version of the code with respect to older RBHT calculations [12]. The deposition rate model  $\Gamma_D$  is described in [12].

Droplet size  $\delta$  is calculated as the minimum of three correlations  $\delta_0, \delta_1, \delta_2$ :

$$\delta = B_r \min(\delta_0, \delta_1, \delta_2) \quad (7)$$

Diameter  $\delta_0$  corresponds to the stability limit of the droplet, based on the Weber number [19]:

$$\text{We} = \frac{\rho_g \Delta V \delta_0}{\sigma} = 8 \quad (8)$$

The Weber number is calculated using the velocity difference  $\Delta V = V_g - V_l$  in case of the 6-equation model, where  $V_g$  and  $V_l$  are respectively the gas velocity and the liquid velocity, including both the continuous liquid and the droplets contributions, and  $\Delta V = V_g - V_{ld}$  in case of the 3-field model, where  $V_{ld}$  is the droplet velocity. When the continuous liquid field and droplet field coexist, droplet diameters estimated by the three-field model can be significantly different to those calculated by the 6-equation model, due the difference of the velocities between the droplets, entrained by the vapor, and the continuous liquid field. Diameter  $\delta_1$ , based on the Laplace scale, is the maximum size of droplet that can be entrained from a mixture level:

$$\delta_1 \propto \sqrt{\frac{\sigma}{g\Delta\rho}} \quad (9)$$

Diameter  $\delta_2$  depends on the droplet volume fraction (or the liquid volume fraction in case of the 6-equation model) is an upper limit useful for flows at very high void fraction. In such conditions, where the latest vanishing part of liquid is supposed to be made of small droplets in the core flow, the interfacial friction diverges while the wall friction becomes negligible and the liquid and gas velocities are equal. For coherence, those latest droplets must be small and this correlation prevents them from being too big. Factor  $B_r$  in equation (7) takes into account the enhancement of droplet break-up due to spacer grids, correlated from PERICLES data. In this revision of the physical models, the break-up factor, depending on the local conditions, is nevertheless calculated in the entire domain of the rod-bundle, and not close to the spacer grids.

### 3. RBHT EXPERIMENTS: DESCRIPTION AND CATHARE MODELING

#### 3.1. RBHT experimental facility & test matrix

The NRC/PSU RBHT experimental loop [20, 21] was built to reproduce the behavior of a PWR post-LOCA core in reflooding condition. Widely instrumented, it provides a certain amount of data on the essential characteristics of these flows. The system is made of a boiler, an injection water supply tank, a test section with upper and lower plenum, carryover tanks, steam separator and pressure oscillation damping tank (see figure 1)

The test section is a 7x7 assembly containing 45 heating rods and 4 unheated rods, all in one flow housing made of Inconel-600. These rods are electrically heated with a bilinear power distribution (the peak being 2.74 m high). Each heater rod has an outer diameter of 9.5 mm and a rod pitch of 12.6 mm. The rods are made of a 3.42 mm diameter cylinder of boron nitride, 1.15 mm of electric coil for the heating system, 1.18 mm of boron nitride, and 0.71 mm of Inconel 600. Along the test section, 7 spacer grids allow the structure to be maintained.

The instrumentation includes 256 thermocouples mounted inside the heater rods, as well as 22 differential pressure cells and 13 stand-off penetrations for pressure drop and vapor temperature measurement. A

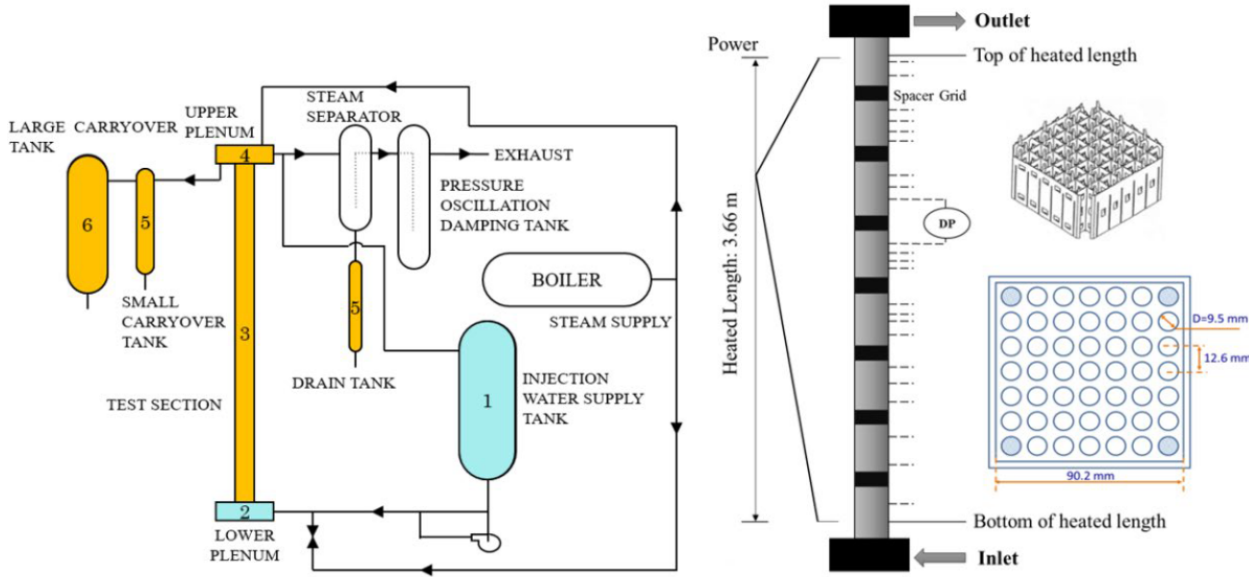


Figure 1. The RBHT facility [21]

Table I. RBHT Experimental Conditions

EXP	Pressure (kPa)	Velocity (cm/s)	Bundle Power (kW)	Subcooling (K)	Reflow Temperature (K)
9005	275	4.97	144.8	9.6	1000
9011	275	8 (for 15 s) 5 (for 15 s) 3 (for 10 s) 1.2 (for 1450 s) 1.14 (for 600 s)	144.8	27	1000
9012	275	2.5 ± 2.5	144.9	9	1000
9014	275	14.94	252.7	80	1144
9015	275	15.34	252.8	11.7	1144
9021	275	2.47	144.9	10	1000
9026	275	2.5	144.6	78.9	1000
9027	275	2.48	144.6	31.7	1000
9029	275	2.59	221.8	47.8	1000
9037	275	5.03	144.6	10.7	1000
9043	275	0.526	34.9	2.8	922

device of 6 pairs of quartz windows makes it possible to visualize the flow. This device is able to generate data on liquid droplet velocity and size distribution in the vapor flow.

In the frame of the OECD benchmark, 11 open tests have been carried out on the RBHT test facility at a nominal pressure of 275.8 kPa. Before the start of reflooding, a preheating phase is carried out to reach the desired temperature. Afterwards, subcooled liquid is injected into the test section, according to the data described in the Table I. A wide range of conditions are tested (constant, stepping down, and oscillatory flow rate).

### 3.2. CATHARE modelling approach

For this study, the RBHT test section is modeled using a 1D module. A single channel is defined with the average geometric characteristics of the bundle (see Figure 2).

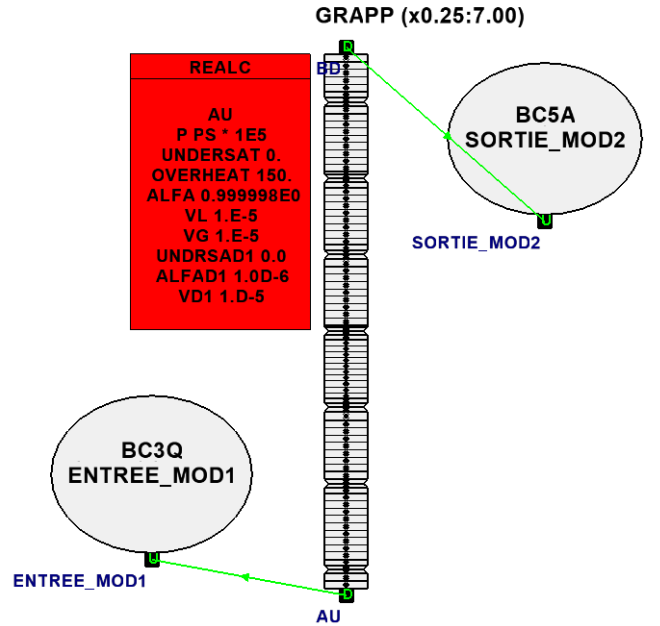


**Figure 2. 1D Nodalization of the Experimental Bundle with CATHARE-3**

The inlet flow rate is assumed homogeneous and lateral phenomena are neglected. In the streamwise direction, the channel is made of 84 cells, refined around the spacer grids. Between the grids, cells have an average thickness of 0.05 m against 0.025 m at grid elevations.

The heating rods are modeled as an internal wall including a radial mesh of four layers (corresponding to the succession of materials) in order to correctly resolve the energy diffusion in the heating element. The bilinear power profile is applied according to the law given by the experimental data. On the other hand, the outer wall of the test section is not modeled and no heat losses are considered. Upper and lower volumes are also ignored.

The spacer grids are taken into account as an element reducing the cross-section in the bundle. In addition, singular pressure loss are added for each grid in accordance with the specifications provided.

In order to obtain the experimental conditions at the rewetting start, the CATHARE calculations are preconditioned. First, the system is initiated with a overheat of 150 K for the steam. This choice was determined a posteriori, in order to impose the conditions as close as possible to the experimental data at  $t = 0s$  (start of reflooding). The heating rods release a power of 8.5 kW until the peak clad temperature (PCT) reaches 621°C. Then, the power of the specific test case is imposed until the PCT reaches the threshold temperature corresponding to the reflow start. For this step, the heat transfer coefficient of vapor convection is empirically modified to ensure the good kinetic behavior (this modification is removed at the reflow start). The tests are then carried out under nominal conditions (flow rate and pressure measurements are not used) using CATHARE's two-fluid model and three-field model separately.

**Table II. Error on PCT features for all open tests simulations. The color code depends on the quality criteria of the results (defined collectively within the benchmark framework): red for poor results, orange for fair results, yellow for good results, and green for excellent results.**

Case	Error on PCT [K]		Error on PCT position [m]		Error on PCT time [s]	
	2-fields	3-fields	2-fields	3-fields	2-fields	3-fields
9005	-32	-29	+0.17	+0.17	-5	-4.6
9011	-45	-20	+0.07	+0.07	+10	-57
9012	-85	-16	+0.02	+0.07	-84	-11
9014	-19	-23	+0.17	+0.17	-2	-3
9015	-26	-24	+0.02	+0.02	-4	-2
9021	-68	-1	+0.02	+0.07	-73	-1
9026	-84	-31	+0.02	+0.07	-24	-29
9027	-69	-2	+0.02	+0.07	-58	-8
9029	-61	+5	+0.02	+0.07	-15	+35
9037	-24	-22	+0.17	+0.17	-7	-6
9043	+14	+10	+0.33	+0.23	+11	-25
Mean error	-46	-14	+0.08	+0.09	-19	-7
RMS	54	20	0.12	0.11	39	22
Characterization	Fair	Good	Excellent	Good	Good	Excellent

#### 4. SIMULATION RESULTS

This section presents simulation results obtained with both the two-fluid 6-equation model (also called 2-fluid model in this part) and the 3-field model of CATHARE 3 V2.1 on the 11 open tests of the benchmark.

##### 4.1. Clad Temperature and wall heat transfer

For safety issues, the rod temperatures and particularly the peak clad temperature (PCT) must be precisely predicted. All the results concerning the PCT (time location, elevation, value) are presented in Table II. The PCT, which varies experimentally between 750 and 950 K, is well predicted by CATHARE. However, a clear difference should be noted between the two-fluid model and the three-field model. The two-fluid model underestimates the PCT by 20 to 80 K depending on the case (mean error of 46 K), while the three-field model reduces the mean error to around 14 K (the root mean square error is also reduced from 54 K to 20 K with the three-field model). Considering the quality criterion of the results (defined collectively within the framework of the benchmark), the results of the two-fluid model are fair whereas those of the 3-field model are good. This trend is confirmed with the prediction of the PCT time. The CATHARE code manages to estimate this quantity fairly precisely. Excellent results are obtained with the 3-field model. The PCT elevation is however overestimated for both models. This error can partly be explained by the modeling choice. 3D modeling of the assembly could provide some clarification on that matter.

**Table III. Selected Open Tests for Code Validation on non-constant flooding rate**

Exp. ID	Pressure (kPa)	Flooding Rate (cm/s)	Peak Power (kW/m)	Inlet subcooling (K)
9027	275.8	2.5	1.31	31.7
9012	275.8	2.5 ± 2.5 Period: 4 s	1.31	9.
9011	275.8	8 (for 15 s) 5 (for 15 s) 3 (for 10 s) 1.2 (for 1450 s) 1.14 (for 600 s)	1.31	26.1

#### 4.2. Validation of non constant flooding rate condition (oscillating and step-down tests)

Table III shows a subset of the open tests selected for the validation of non constant flow rate situation. Case 9027 has a constant flooding rate, serving as the baseline case for comparison. Exp. 9012 has an oscillatory inlet velocity condition with a 2.5 cm/s base component and  $\pm 2.5$  cm/s oscillatory component. The oscillation period is 4 s. Exp. 9011 is a step-down test with the liquid inlet velocity being gradually reduced from 8 cm/s to 1.14 cm/s. Figures 3,4,5,6,7 and 8 show the results of CATHARE for these selected cases for key variables of reflooding (respectively the quenching front, a rod temperature signal, a vapor temperature signal, droplet size, carryover fraction and overall pressure loss in the bundle).

We observe a better estimate of the figure of merits by the three-field model, on all cases. The most marked improvement is obtained on the rod temperature profiles (Figure 4). At 2.69 m, the good prediction of the 3-field model is noticeable. It manages to reproduce precisely the shape and the amplitude of the experimental profiles, improving the assessment of PCT features as developed in the previous section. On the other hand, at 2.89 m (not shown here), there is a tendency of the CATHARE code to overestimate the clad temperatures. The prediction seems optimal as long as the power profile increases with elevation. The three-field model is also more efficient on the prediction of the carryover fraction and pressure losses (Figures 7 and 8)

Regarding non-constant flow rate condition, CATHARE does not show any particular behavior. Whether in oscillating (case 9012) or step-down tests (case 9011), CATHARE obtains results similar to those at constant flow rate (case 9027). These results are encouraging on the code capacity to manage real conditions in industrial transient.

The results on the droplet diameter are also fair. In CATHARE simulations, the droplet diameter tends to increase with elevation. Indeed, it is related to the relative velocity between phases, increasing as the drops accelerate along the bundle (see equation (8)). CATHARE does not have a model allowing locally an effect of the spacer grids on the drop diameter, although the break-up of droplets due to the grids is taking into account.

In figure 5, the difference observed for the droplet diameter between the 2-field and the 3-field models is due to the relative velocity, higher in the 2-field model than in the 3-field model, in the considered RBHT conditions. This relative velocity is used in the formulation of the droplet diameter model equation (8). As a consequence, due to the formulation 7, the droplet diameter is determined by the hydrodynamic

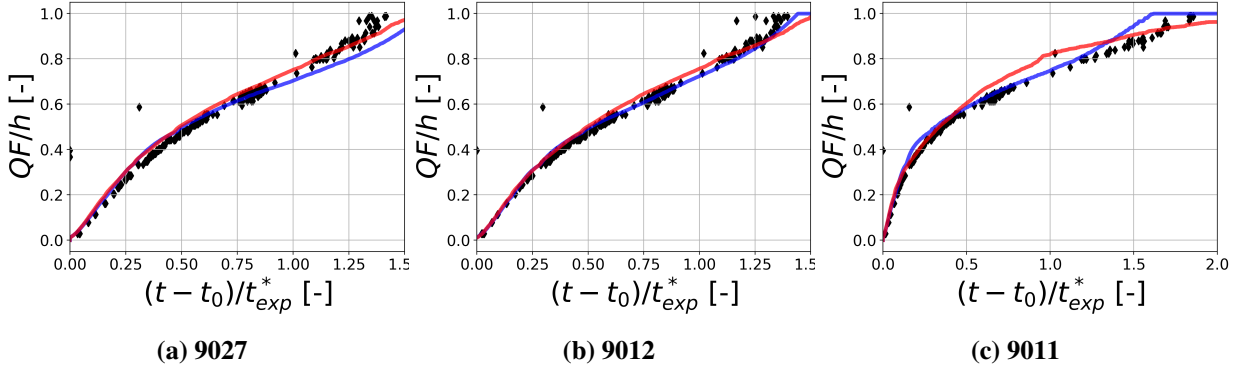


**Figure 3. Normalized quench front vs. dimensionless time for experiment (black line) and numerical simulations of CATHARE 3 with 2-field (blue line) and 3-field (red line) models.  $t_{exp}^*$  is a characteristic time of the experiment,  $t_0$  corresponds to the reflood start and  $h$  is the height of the test section. At  $t < 0s$ , the quench front is at  $z = 0m$ .**

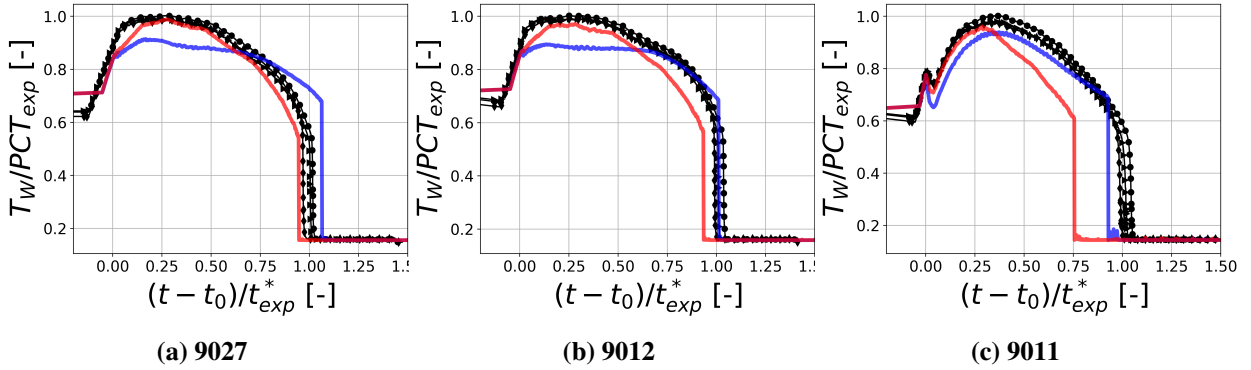


**Figure 4. Normalized rod temperature vs. dimensionless time at 2.69 m for experiment (black line) and numerical simulations of CATHARE 3 with 2-field (blue line) and 3-field (red line) models.  $t_{exp}^*$  is a characteristic time of the experiment,  $t_0$  corresponds to the reflood start and  $PCT_{exp}$  is the experimental value of the PCT. The time before  $t = 0s$  is added to see the heated phase of the initialization and compare with the experimental data.**

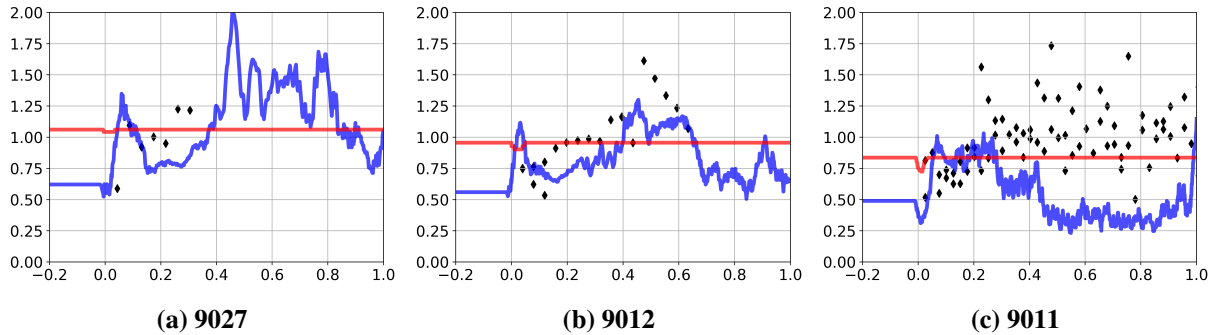


**Figure 5. Normalized droplet diameter vs. dimensionless time at the fifth grid elevation for experiment (black line) and numerical simulations of CATHARE 3 with 2-field (blue line) and 3-field (red line) models.  $t_{exp}^*$  is a characteristic time of the experiment.**

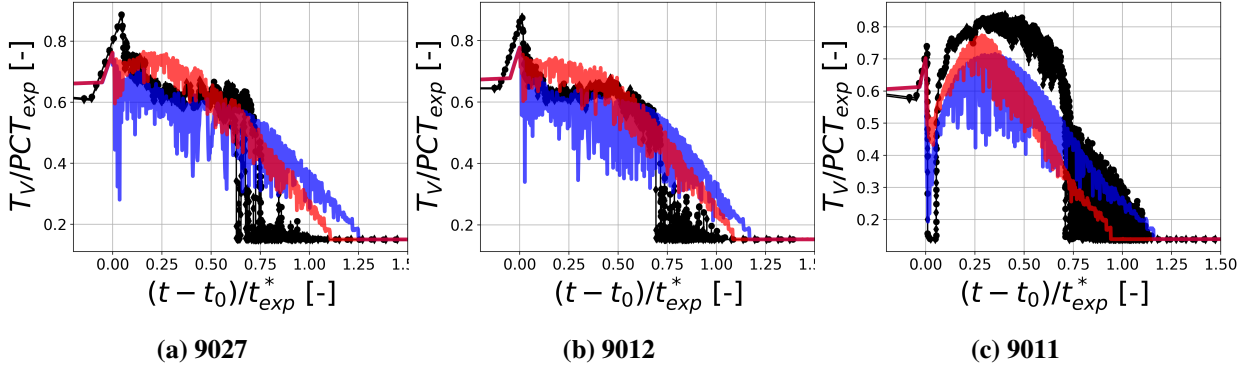


**Figure 6.** Normalized vapor temperature vs. dimensionless time at 2.93m for experiment (black line) and numerical simulations of CATHARE 3 with 2-field (blue line) and 3-field (red line) models.  $t_{exp}^*$  is a characteristic time of the experiment and  $PCT_{exp}$  is the experimental value of the PCT. The time before  $t = 0s$  is added to see the heated phase of the initialization and compare with the experimental data.

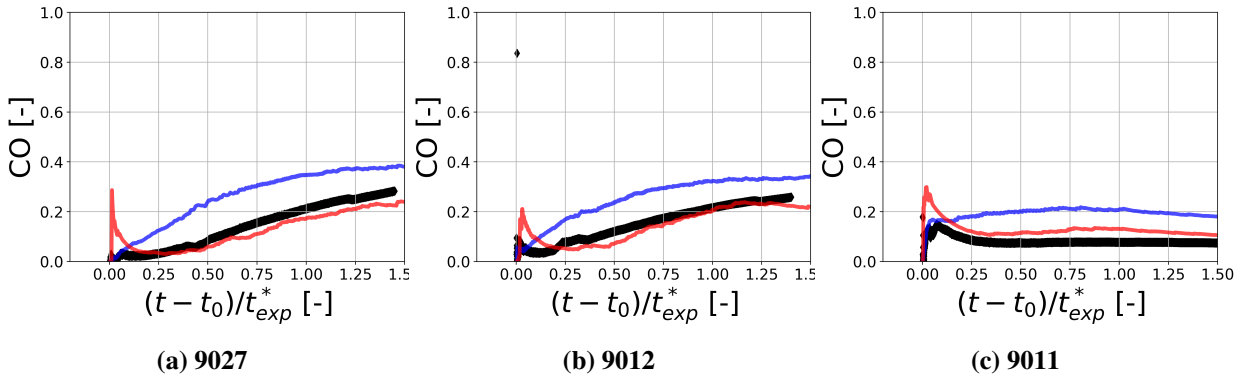


**Figure 7.** Carryover fraction vs. dimensionless time for experiment (black line) and numerical simulations of CATHARE 3 with 2-field (blue line) and 3-field (red line) models.  $t_{exp}^*$  is a characteristic time of the experiment.

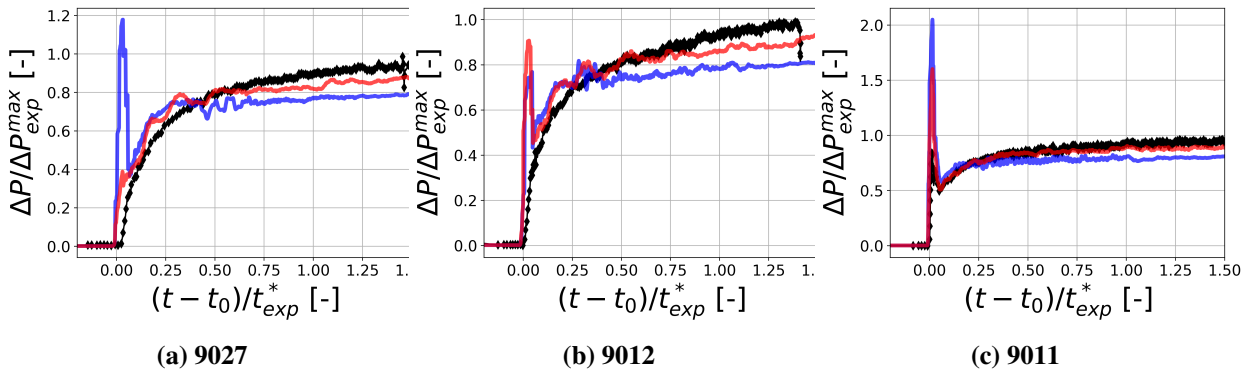


**Figure 8.** Pressure loss in the bundle vs. dimensionless time for experiment (black line) and numerical simulations of CATHARE 3 with 2-field (blue line) and 3-field (red line) models.  $t_{exp}^*$  is a characteristic time of the experiment.

**Table IV. Selected Open Tests for Code Validation on different flooding rate**

Exp. ID	Pressure (kPa)	Flooding Rate (cm/s)	Peak Power (kW/m)	Inlet subcooling (K)
9043	275.8	0.53	0.32	2.8
9027	275.8	2.5	1.31	31.7
9014	275.8	14.9	2.3	80

instability linked to the Weber number and to the properties of the flow (velocity) in case of the two-fluid model, while in three-field model, it is determined by the capillary instability (which only depend on physical properties of the water, explaining why the droplet diameter has a constant value). The role of the interfacial friction should be investigated.

The vapor temperature results from a balance between wall heat transfer (convection / radiation) and interfacial heat transfer with the droplets (convection / vaporization). A sensitivity analysis shows that the vapor temperature is not really sensitive to heat transfer with the wall, and that it is greatly impacted by the heat transfer at the interface of the drops. Droplet diameter being known in the RBHT facility, calculations with imposed diameters have been carried out. It was first concluded that the differences concerning the vapor temperature (between 2-field and 3-field models) does not come from different estimation of the droplet diameter but from the void fraction prediction. In the two-fluid model, the drop-to-vapor heat transfer  $q_{ve}$  depends directly on the void fraction which leads the regime transition between Inverted Annular Film Boiling (IAFB) and Dispersed Flow Film Boiling (DFFB):

$$q_{ve} = (1 - \omega_{\alpha})q_{veIAFB} + \omega_{\alpha}q_{veDFFB} \quad (10)$$

where  $\omega_{\alpha}$  is a function of the void fraction  $\alpha$  which approach 1 when the void fraction approach 1. With the two-fluid model the void fraction upstream of the quench front is 0.9 against 0.7 for the three-field model. Thus, with  $\alpha = 0.9$ , the two-fluid model leads to a DFFB regime (the heat transfer then increases with the interfacial area), explaining why the vapor temperature is generally smaller than in the 3-field model. In 3-field model, the distinction between dispersed and continuous phases allows to dispense with this transition criterion. For small and moderate liquid flow rate, the results of the three-field model are slightly better.

### 4.3. Discussion

The CATHARE code has shown on these open tests an ability to take into account non-constant flow conditions (one of the main challenges of the benchmark). However, other limitations were found. In particular, for moderate flooding rate (here around 2.5 cm/s), CATHARE shows very good results. This is not the case for lower and higher flooding rate. In table IV, we have selected three tests to highlight this effect, and provide some idea for a possible improvement of the code.

The propagation of the quench front (figure 9) is sensitive to many parameters (film boiling, forced convection, total heat transfer, droplet diameter, interfacial friction, film sputtering model, droplet pullout). In Figure 9, the propagation of the quench front is too fast for cases at low liquid flow rate (9043) and high liquid flow rate (9014). For the cases with intermediate flow rate, quench fronts are well predicted, whether in two fields or in three fields model. In cases where the front is not ideally resolved, the rod and steam temperatures are however in fair agreement with experiment (see for instance figure 10).

For higher flooding rate, the experimental steam temperature decreases sharply from the start of reflow,

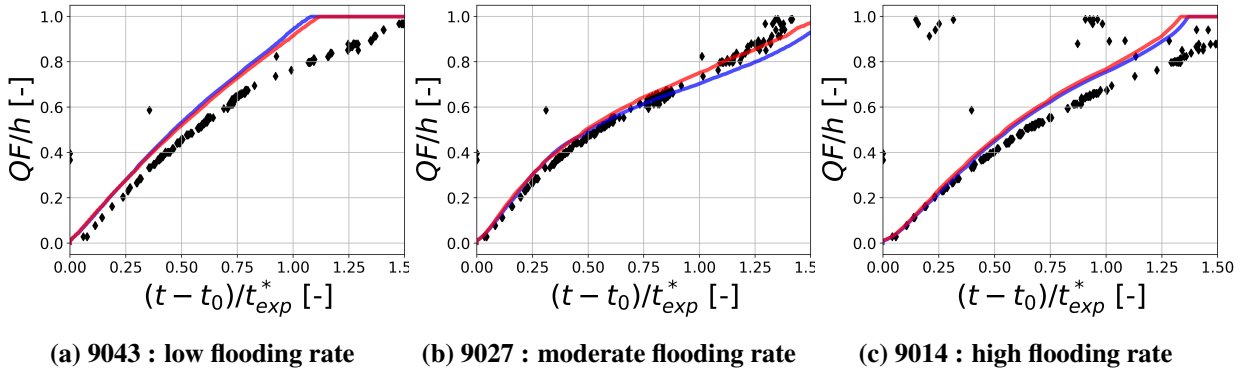


**Figure 9.** Normalized quench front vs. dimensionless time for experiment (black line) and numerical simulations of CATHARE 3 with 2-field (blue line) and 3-field (red line) models.  $t_{exp}^*$  is a characteristic time of the experiment,  $t_0$  corresponds to the reflood start and  $h$  is the height of the test section. At  $t < 0s$ , the quench front is at  $z = 0m$ .

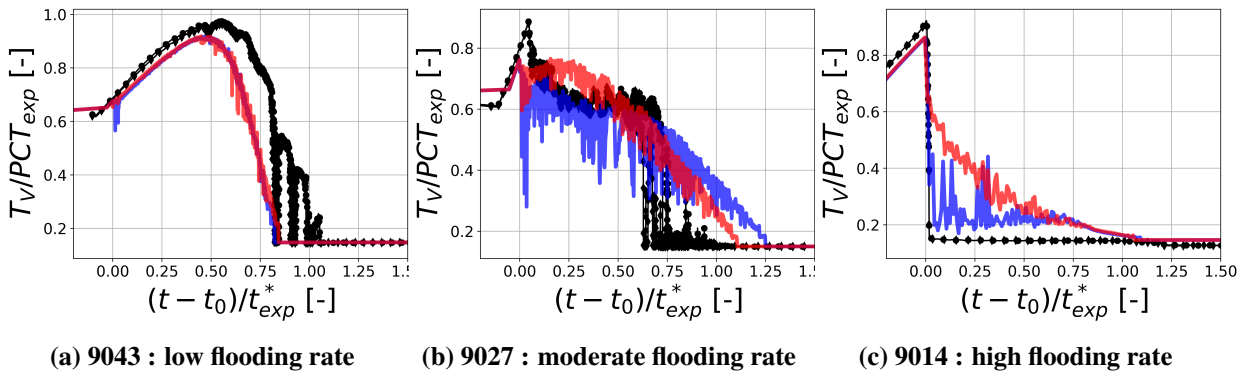


**Figure 10.** Normalized vapor temperature vs. dimensionless time at  $2.93m$  for experiment (black line) and numerical simulations of CATHARE 3 with 2-field (blue line) and 3-field (red line) models.  $t_{exp}^*$  is a characteristic time of the experiment and  $PCT_{exp}$  is the experimental value of the PCT. The time before  $t = 0s$  is added to see the heated phase of the initialization and compare with the experimental data.

even downstream from the quench front (see case 9014 in figure 10). Physically, this phenomenon may be explain by a violent ejection of fine droplets due to the phenomenon of film sputtering. The two-fluid model captures this phenomenon relatively well. It predicts a high relative velocity between the phases. Then, the droplet diameter drastically decreases when  $|V_g - V_l|$  grows and the drop-to-interface heat transfer  $q_{le} \propto 1/\delta^2$  increases (the relative velocity of droplets represents a weighted average between the relative velocity of the continuous liquid core and the relative velocity of the drops; this lack of distinction in the two-field model can be the source of significant error). However, it explains the good results for the two-fluid model on cases with high flooding rates but this result appears to be the consequence of error compensation. Indeed, the start of reflood coincides with a sudden increase in the pressure drop in the case of the two-field model (see for instance case 9027 in figure 8). This pressure variation (too large compared to the experiment) is mainly due to the large quantity of liquid in the bundle which increases the hydrostatic loss. On the other hand, the three-field model follows the experimental pressure drop better, suggesting that the quantity of drops ejected in that case is more realistic. Thus, the poor estimate of the vapor temperature with the three-field model (for high flooding rate cases) requires further analysis.

## 5. CONCLUSIONS

The results of the CATHARE 3 V2.1 code on the 11 open-tests of the RBHT benchmark are relatively good. The three-field model (partly calibrated on previous RBHT tests) gives better results than the two-fluid model on several key quantities (pressure, temperature, PCT, carryover fraction). One of the challenges of the benchmark, namely testing non-constant flooding rate conditions, has given satisfactory results. The CATHARE code succed to handle oscillating and variable flow conditions. The comparison with the experimental results, as well as the sensitivity analysis carried out on some models, allow considering several improvements for the future.

- On the film boiling model to improve the velocity of quench front propagation at high liquid flow rates
- On the droplet diameter model to improve the prediction of the vapor temperature at high liquid flow rates.

These analyzes will require further study. The next blind tests will allow, among other things, to confirm the present observations in order to consider the future actions to be carried out.

## ACKNOWLEDGMENTS

This work has been carried out in the framework of the NEPTUNE project, funded by CEA, EDF, Framatome and IRSN.

## REFERENCES

1. P. Emonot, A. Souyri, J. Gandrille, and F. Barré, “CATHARE-3: A new system code for thermal-hydraulics in the context of the NEPTUNE project,” *Nuclear Engineering and Design*, **241**, pp. 4476–4481 (2011)
2. A. Janicot, J. Bartak, and T. Haapaetho, “Recent developments in reflood modelling with CATHARE,” *Proc. Int. Conf. on New trends in Nuclear System Thermohydraulics*, Pisa, Italy, (1994)

3. J. Kelly, J. Bartak, and A. Janicot, "Reflood modelling under oscillatory flow conditions with CATHARE," *Proc. NURETH-6*, Grenoble, France, (1993)
4. OECD, "Post-BEMUSE Reflood Model Input Uncertainty Methods (PREMIUM) Benchmark - Final Report," Report NEA/CSNI/R(2016)18, OECD (2017)
5. C. Morel and P. Boudier, "Validation of the CATHARE code against PERICLES 2D reflooding tests," *Proc. NURETH-9*, San Francisco, CA, USA, (1999)
6. I. Dor and P. Germain, "Core radial power profile effect during Reflooding - Validation of CATHARE2 3D module using SCTF tests," *Proc. NURETH-14*, Toronto, Canada, (2011)
7. J. Bartak, D. Bestion, and T. Haapalehto, "The top-down reflooding model in the CATHARE code," *Nuclear Engineering and Design*, **141**, pp. 141–152 (1994)
8. S. Jayanti and M. Valette, "Prediction of dryout and post-dryout heat transfer at high pressures using a one-dimensional three-fluid model," *Heat and Mass Transfer*, **47** (22), pp. 4895–4910 (2004)
9. M. Spirzewski, P. Fillion, and M. Valette, "Prediction of annular flows in vertical pipes with new correlations for the CATHARE-3 three-field model," *Proc. NURETH-17*, Xi'an, China, (2017)
10. M. Spirzewski and H. Anglart, "An improved phenomenological model of annular two-phase flow with high accuracy dryout prediction capability," *Nuclear Engineering and Design*, **331**, pp. 176–185 (2018)
11. S. Jayanti and M. Valette, "Calculation of dry out and post-dry out heat transfer in rod bundles using a three field model," *Heat and Mass Transfer*, **48** (9), pp. 1825–1839 (2005)
12. M. Valette, J. Pouvreau, D. Bestion, and P. Emonot, "Revisiting large break LOCA with the CATHARE-3 three-field model," *Nuclear Engineering and Design*, **241**, pp. 4487–4496 (2011)
13. S. Lutsanych, F. Moretti, and F. D'Auria, "Validation of the CATHARE 1-D and 3-D reflood models against FEBA and ACHILLES experimental tests," *Nuclear Engineering and Design*, **321**, pp. 266–277 (2017)
14. P. Fillion, "Development of the CATHARE 3 three-field model for simulations in large diameter horizontal pipes," *Proc. NURETH-18*, Portland, OR, USA, (2019)
15. C. Housiadas, J. Veteau, and R. Deruaz, "Two-dimensional quench front progression in a mul-assembly rod-bundle," *Nuclear Engineering and Design*, **113**, pp. 87–98 (1989)
16. G. Yadigaroglu et al., "Modeling of reflooding," *Nuclear Engineering and Design*, **145**, pp. 1–35 (1993)
17. P. Berenson, "Film-boiling heat transfer from a horizontal surface," *Journal of Heat Transfer*, **83** (3), pp. 351–358 (1961)
18. M. Yuen and L. Chen, "Heat-transfer measurements of evaporating liquid droplets," *International Journal of Heat and Mass Transfer*, **21** (5), pp. 537–542 (1978)
19. D. Bestion, "The physical closure laws in the CATHARE code," *Nuclear Engineering and Design*, **124**, pp. 229–245 (1990)
20. E. R. Rosal, T. F. Lin, I. S. McLellan, and R. Brewer, "Rod Bundle Heat Transfer Facility Description Report," NUREG/CR-6976, ML102290227, US NRC (2010)
21. S. M. Bajorek and F.-B. Cheung, "Rod Bundle Heat Transfer Thermal-Hydraulic Program," *Nuclear Technology*, **205** (1-2), pp. 307–327 (2018)